



AMS
American Meteorological Society

Supplemental Material

Bulletin of the American Meteorological Society

The Summer Heatwave 2022 over Western Europe: An Attribution to Anthropogenic Climate Change

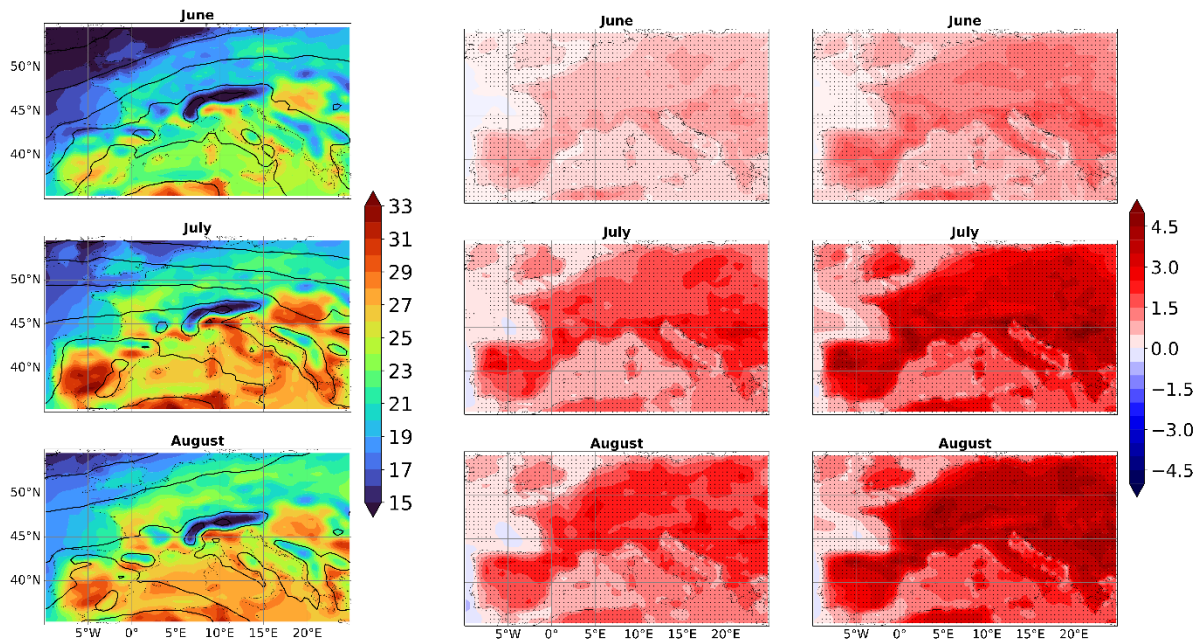
<https://doi.org/10.1175/BAMS-D-24-0017.1>

© [Copyright 2024 American Meteorological Society](#) (AMS)

For permission to reuse any portion of this work, please contact permissions@ametsoc.org. Any use of material in this work that is determined to be “fair use” under Section 107 of the U.S. Copyright Act (17 USC §107) or that satisfies the conditions specified in Section 108 of the U.S. Copyright Act (17 USC §108) does not require AMS’s permission. Republication, systematic reproduction, posting in electronic form, such as on a website or in a searchable database, or other uses of this material, except as exempted by the above statement, requires written permission or a license from AMS. All AMS journals and monograph publications are registered with the Copyright Clearance Center (<https://www.copyright.com>). Additional details are provided in the AMS Copyright Policy statement, available on the AMS website (<https://www.ametsoc.org/PUBSCopyrightPolicy>).

1 **Supplementary for ‘The summer heatwave 2022 over Western Europe: An**
2 **attribution to anthropogenic climate change’**

3



4

5 **Figure 1s**

6 *The left column shows the 2m temperatures [°C] (shaded) and present-time geopotential height at*
7 *500hPa [m] (black contour lines) of the European heatwave 2022 for JJA. The middle column shows the*
8 *differences in 2m temperature [°C] between the present-time and preindustrial simulations and the*
9 *right column the differences between +2°C and preindustrial simulations as shaded fields. Stippling*
10 *indicates where all present-time or +2°C members are > 0.1°C above all preindustrial members for that*
11 *grid point.*

12

13 **Spectrally nudged storylines**

14

15 The aim of this article is to find the effect of anthropogenic climate change on a specific weather event,
16 the 2022 European heatwave. To do so we need a method that can provide viable knowledge on such
17 a narrow time scale. The commonly applied statistical approaches (also known as the frequentist
18 approach) cannot provide this, since they need a large number of events to produce any answers of
19 statistical meaning. In the frequentist approach, the events in free running simulations are selected
20 based on roughly the same location and, in the case of a heatwave, the temperature averaged over
21 space and time (e.g. duration of heatwave) and are grouped to an event class. The technique is thus
22 used to attribute an event type instead of a specific event (Watanabe et al. 2013). Also, attributing the

23 atmospheric dynamics of an extreme event comes with large uncertainties, not rarely larger than a
 24 random attribution (Shepherd 2014). Interpreting such highly uncertain results is difficult.
 25 Nonetheless, understanding the changing probabilities of extreme weather is crucial information for
 26 e.g. risk assessment and policy making, and therefore the statistical methods are much needed and
 27 important.

28
 29 However, probabilities are not the focus of this study. Instead, it is meant to answer the question ‘How
 30 much did the intensity of this extreme event change due to anthropogenic climate change?’ To do so,
 31 we use the spectrally nudged storyline approach as described in van Garderen (2022). In this approach
 32 the dynamical situation of the specific extreme weather event is re-simulated with different
 33 climatological background, either with less than, equal to or more than present day levels of global
 34 warming. Doing so the effect of climate change on a specific extreme weather event can be quantified
 35 based on known thermodynamic aspects. The results presented in this study are thus a conditional
 36 attribution, since the dynamic situation is nudged towards observed weather patterns which occurred
 37 at the time of the heatwave. This provides insight into the thermodynamic climate change signal that
 38 otherwise might have been lost in the uncertainty noise of the dynamic signal. Moreover, it enables a
 39 quantitative attribution of a specific extreme weather event. Differences between the frequentist and
 40 storyline approach are summarized in Table 1s, please note that the table is not meant to be an
 41 exhaustive overview.

42

Spectrally Nudged Storylines Approach	Frequentist Approach
Specific extreme event	Extreme event class
Quantitative results	Probabilistic results
Conditional	Unconditional
Uncertainty based on thermodynamics	Uncertainty based on dynamics
Requires limited number of conditioned (spectrally nudged) simulations	Requires large number of free running model simulations

43

44 **Table 1s**

45 *Comparison of extreme event attribution based on the spectrally nudged storyline approach and the*
 46 *frequentist approach.*

47

48 **SST warming pattern**

49

50 To compute the changes in sea surface temperature (SSTs) for the preindustrial and +2°C storylines,
51 SST warming patterns were computed. For the preindustrial simulations, this pattern is constructed
52 based on 2015-2024 Max Planck Institute Earth System Model MPI-ESM1.2-HR (Müller et al. 2018)
53 SSP370 scenario data minus preindustrial PiControl simulations from 2015-2024. This warming pattern
54 is then subtracted from the NCEP SSTs. This way the reanalyzed SST pattern, reduced by the warming
55 pattern, is still generally existent and it is possible to simulate weather patterns, which are close to
56 reality. The greenhouse gas (GHG) levels were set to preindustrial values. For the +2°C simulations the
57 difference between CMIP6 MPI-ESM1.2-HR (Müller et al. 2018) SSP585 scenario members for the
58 averaged period 2045-2054 and the averaged historical reference period 1850 to 1920 was computed,
59 which resulted in a +2°C warmer world. This warming pattern was then added to the NCEP SSTs. The
60 GHG levels were accordingly selected for the 2045-2054 period. The spectrally nudged storylines were
61 then computed with ECHAM6 using NCEP SSTs and GHG levels for the present time and using the
62 changed SSTs and GHG levels for the preindustrial and +2°C warmer world.

63

64 ***Simulated Annealing and Diversified Randomization (SANDRA)***

65

66 SANDRA (Philipp et al. 2007) is a non-hierarchical clustering technique based on conventional k-means
67 clustering. In this study, SANDRA is used on temperature anomaly fields with negative anomalies being
68 omitted, so that the focus of the clustering is purely on heatwaves. SANDRA attempts to group the
69 input fields into a predefined number of clusters, such that the differences between fields in one
70 cluster (intra-cluster variability) are minimized, and the differences between different clusters (inter-
71 cluster variability) are maximized. Differences are measured by the Euclidean distances between the
72 fields. The specific number of clusters chosen in this study shows a good balance between the intra-
73 and inter-cluster variability.

74

75 In the process of assigning fields to clusters, the process of simulated annealing that is implemented
76 in SANDRA allows the overall data partitioning quality to be temporarily decreased, but in the final
77 partitioning, the clusters are closer to the 'global optimum' than, e.g., in standard k-means clustering.
78 SANDRA has been developed for clustering atmospheric circulation fields (e.g. sea level pressure or
79 geopotential height) and has shown good or even superior performance compared with other
80 clustering methods for various applications, also in terms of computational effort. To our knowledge,
81 the application of SANDRA to the context of heatwaves is novel.

82

83 In the resulting set of heatwave clusters, the dominant one (i.e., the one with most members) is the
84 non-heatwave cluster (value of zero basically all over the domain; not shown). This is consistent with
85 our understanding of heatwaves being extreme events, i.e. being exceptions from the climatological
86 state.

87

88 The basic set of heatwave clusters for this study is computed from ERA5 reanalysis data following the
89 procedure outlined above. For a comparison with the longer paleo-climate period, we assign each
90 field (positive temperature anomalies as for ERA5) from the long MPI-ESM past2k simulation to the
91 clusters obtained from ERA5: for each of the model fields, the difference to each of the ERA5 heatwave
92 clusters is measured by the Euclidean distance between the cluster and the field. The respective day
93 is then assigned to the cluster with the smallest distance.

94

95 ***MPI-ESM_past2k simulation***

96

97 The paleo simulation employed in this study uses the Max Planck Institute Earth System Model (MPI-
98 ESM) in the configuration for paleo-applications (MPIESM-P) according to the Paleoclimate Modelling
99 Intercomparison Project, phase 3 (PMIP3) protocol (Jungclaus et al. 2014). The atmosphere model
100 ECHAM6 is run at a horizontal resolution of spectral truncation T63 (1.875) with 47 vertical levels. The
101 ocean/sea-ice model MPIOM features a conformal mapping grid with nominal 1.5 resolution and 40
102 vertical levels (GR1.5L40) (Jungclaus et al. 2014).

103

104 The paleo simulation for the years 1 to 2014 was used in order to analyze the very long time span of
105 the last about 2000 years to achieve more reliable statistics on how exceptional the European summer
106 heatwave 2022 was in a historical context. Generally, the past2k simulation should show more decadal
107 or centennial variability than a preindustrial control run as it has more complex forcings (changing
108 land use, volcanic activity, orbital, solar and GHG forcings). The paleo run is therefore supposedly
109 closer to reality for the preindustrial period than a control run with less forcings.

110

111

112 **Literature:**

113

114 van Garderen, L., 2022: Climate change attribution of extreme weather events using spectrally
115 nudged event storylines. PhD Thesis. Staats- und Universitätsbibliothek Hamburg Carl von Ossietzky,
116 <https://ediss.sub.uni-hamburg.de/handle/ediss/9978>.

117

118 Jungclaus, J. H., K. Lohmann, and D. Zanchettin, 2014: Enhanced 20th-century heat transfer to the
119 Arctic simulated in the context of climate variations over the last millennium. *Clim. Past*, **10**, 2201–
120 2213, <https://doi.org/10.5194/cp-10-2201-2014>.

121

122 Müller, W. A., and Coauthors, 2018: A Higher-resolution Version of the Max Planck Institute Earth
123 System Model (MPI-ESM1.2-HR). *J. Adv. Model. Earth Syst.*, **10**, 1383–1413,
124 <https://doi.org/10.1029/2017MS001217>.

125

126 Philipp, A., P. M. Della-Marta, J. Jacobeit, D. R. Fereday, P. D. Jones, A. Moberg, and H. Wanner, 2007:
127 Long-Term Variability of Daily North Atlantic–European Pressure Patterns since 1850 Classified by
128 Simulated Annealing Clustering. *J. Clim.*, **20**, 4065–4095, <https://doi.org/10.1175/JCLI4175.1>.

129

130 Shepherd, T. G., 2014: Atmospheric circulation as a source of uncertainty in climate change
131 projections. *Nat. Geosci.*, **7**, 703–708, <https://doi.org/10.1038/ngeo2253>.

132

133 Watanabe, M., H. Shiogama, Y. Imada, M. Mori, M. Ishii, and M. Kimoto, 2013: Event Attribution of
134 the August 2010 Russian Heat Wave. *Sola*, **9**, 65–68, <https://doi.org/10.2151/sola.2013-015>.

135

136